Journal of Alloys and Compounds 515 (2012) 4–7

Contents lists available at SciVerse ScienceDirect

Journal of Alloys and Compounds

journal homepage: www.elsevier.com/locate/jallcom

Letter

4-nm thick multilayer structure of multi-component (AlCrRuTaTiZr)N_x as robust diffusion barrier for Cu interconnects

Shou-Yi Chang[a,*], Chen-En Li[a], Sheng-Cheng Chiang[a], Yi-Chung Huang[a,b]

[a] *Department of Materials Science and Engineering, National Chung Hsing University, Taichung 40227, Taiwan*
[b] *Central Regional Instrument Center, National Chung Hsing University, Taichung 40227, Taiwan*

ARTICLE INFO

Article history:
Received 23 September 2011
Accepted 20 November 2011
Available online 30 November 2011

Keywords:
Diffusion barrier
Multi-component
Multilayer

ABSTRACT

This work develops a multilayer structure of alternating (AlCrRuTaTiZr)$N_{0.5}$ senary nitride and AlCrRuTaTiZr senary alloy with a total thickness of only 4 nm as a diffusion barrier layer for application to Cu interconnects. Under annealing at a high temperature of 800 °C, the interdiffusion of Cu and Si through the multilayer structure was effectively retarded without the formation of any Cu silicides. Interdiffusion occurred only at 900 °C, and compounds that included Cu_3Si were thus formed. This finding suggests that the high endurance temperature of the diffusion barrier is probably attributable to the stable amorphous solid-solution structure, the high packing factor, the severe lattice distortions that are caused by the incorporation of multiple components and the elongated diffusion path through the multilayer stacking structure.

1. Introduction

A highly thermally stable, robust diffusion barrier layer is critical in an interconnect structure to inhibit rapid Cu diffusion and the subsequent formation of silicides [1–3]. Therefore, films of transitions metal nitrides, mainly TiN and TaN, have been developed and extensively used in Al and Cu interconnects, respectively [4,5]. However in the 32 or 22 nm generation of semiconductor manufacturing, a more suitable barrier layer is highly demanded because of the microstructure defects of the conventional barrier materials such as columnar boundaries. Therefore, in recent years, diffusion barriers that comprise ternary elements or layered structures have been extensively studied [6–14]. Barrier systems with ternary or more components, such as Ta–W–N (50 nm thick) [6], Ru–Ti–N (10 nm) [7], Ta–Ge–(O)N (50 nm) [8], and Ru–Ta–N (15 nm) [9], usually have large lattice distortions and an amorphous structure that reduces the number of viable diffusion paths and effectively increases diffusion resistance. Layered (mostly bilayered) structures, including Ti/MoN (5/5 nm) [10], Ir/TaN (5/5 nm) [11], Ru/TaN (5/5 nm; 3/5 nm) [12,13], and atomic-layer deposited Ru/TaCN (12/2 nm) [14], increase diffusion distance by a layer-interface lattice mismatch, enhance diffusion resistance, and strengthen Cu adhesion. Additionally, segregation-induced self-forming barriers (such as Mn [15]) and organic self-assembled monolayers (of NH_2SAM, for example, [16]) have also attracted much interest. However, appropriate ultra-thin barrier layers with a thickness of 3–5 nm but still a high diffusion resistance that meets the strict requirements of the generation below 32 nm have rarely been reported.

Multi-component-induced lattice distortions and layered-structure-increased diffusion distances effectively improve the resistance of barrier layers to Cu diffusion [6–14]. Therefore, owing to the thermodynamically stable solid-solution structures and severe lattice distortions of multiprincipal-element alloys (called high entropy alloys, HEAs) [17–19], individual films and bilayered structures of HEAs and HEA nitrides (denoted as HEANs) with a nanocomposite or amorphous structure and a thickness from 70 to as low as 10 nm have been developed as diffusion barriers [20–22]. These previous studies have shown that the multi-component HEAN and/or HEA-based barrier materials (such as quinary (AlCrTaTiZr)N_x) sustained a high temperature of 800 °C for 30 min inhibiting Cu diffusion; this fact suggests that high stability of the interconnect structures in the thermal cycles in manufacturing (300–400 °C) and operation (100–200 °C) is retained for much longer time. However, the large thickness ($\geq$ 10 nm) of the previously developed barriers limits their range of practical applications. In this investigation, a quaternary-layered (QL) structure with a total thickness of only 4 nm, comprising alternating (AlCrRuTaTiZr)$N_{0.5}$ senary nitride and AlCrRuTaTiZr senary alloy layers (each 1 nm thick), is further developed as a more promising diffusion barrier of the sub-32 nm manufacturing generation.

2. Experimental

The QL structure, comprising alternating (AlCrRuTaTiZr)$N_{0.5}$ senary nitride (bottom) and AlCrRuTaTiZr senary alloy (top) layers, each with a thickness of around

---

[*] Corresponding author. Tel.: +886 4 22857517; fax: +886 4 22857017.
E-mail address: shouyi@dragon.nchu.edu.tw (S.-Y. Chang).

0925-8388/$ – see front matter © 2011 Elsevier B.V. All rights reserved.
doi:10.1016/j.jallcom.2011.11.082

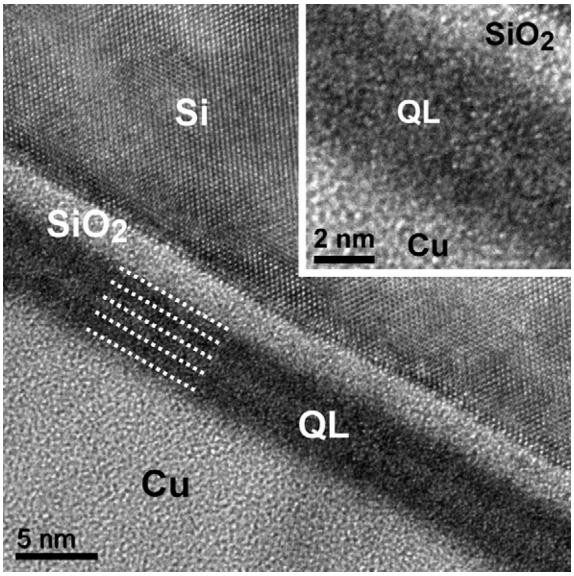

Fig. 1. HRTEM image of as-deposited Si/QL/Cu film stack (insert: magnified image around QL barrier).

1 nm, and with a total thickness of the structure of only 4 nm, was deposited on Si substrates by typical reactive radio-frequency magnetron sputtering. The sputtering target was prepared using equimolar Al, Cr, Ru, Ta, Ti, and Zr (around 16.7 at.% for each element) by vacuum arc-melting the constituent elements, and then cutting and polishing the solidified bulk into a disc with a diameter of 50 mm. The (AlCrRuTaTiZr)$N_{0.5}$ nitride and AlCrRuTaTiZr alloy films were deposited at a plasma power of 150 W and a substrate bias of −100 V at room temperature, in an Ar/N_2 mixed atmosphere and a pure Ar atmosphere, respectively. The total gas flow rate was set to 30 sccm (working pressure 6×10^{-3} Torr); for the deposition of (AlCrTaTiZrRu)$N_{0.5}$, the N_2 flow rate was adjusted to 9 sccm. On the QL barrier, a Cu film with a thickness of 400 nm was deposited at a power of 50 W to obtain a Si/QL/Cu film stack. Thermal annealing of the film stacks at 700–900 °C for 30 min in an N_2/H_2 atmosphere (500 sccm) was performed to study the diffusion resistance of the QL barrier.

The chemical compositions of as-deposited (AlCrRuTaTiZr)$N_{0.5}$ and AlCrRuTaTiZr films were determined by electron probe micro-analyses (EPMA, JEOL JXA-8800 M; film thickness ~500 nm). A scanning electron microscope (SEM, JEOL JSM-6700F) was used to observe the morphologies of the as-deposited and annealed Si/QL/Cu film stacks, and a glancing incident angle (0.5°) X-ray diffractometer (XRD, Rigaku Dmax 2000) was used to analyze the crystal structures. The microstructures and detailed lattice structures of the as-deposited and annealed film stacks were observed using a high-resolution transmission electron microscope (HRTEM, JEOL JEM-3000F). The sheet resistance of the film stacks was measured by a four-point probe station (Keithley 2400).

3. Results and discussion

Table 1 lists the chemical compositions of as-deposited (AlCrRuTaTiZr)$N_{0.5}$ senary nitride and AlCrRuTaTiZr senary alloy films, as determined by EPMA. Except the lower Al contents than the designed values due to a resputtering effect, the contents of the other metallic elements in the AlCrRuTaTiZr alloy and (AlCrRuTaTiZr)$N_{0.5}$ nitride films were approximately 17.2 and 10.8 at.%, respectively–close to the designed compositions and in near-equimolar ratios. Because the content ratio of N to total metallic elements in the nitride film was estimated to be around 0.53 (33.2–62.6 at.%), the nitride is denoted (AlCrRuTaTiZr)$N_{0.5}$. Fig. 1 further presents the HRTEM image of the as-deposited Si/QL/Cu film stack; a stacked structure of the single-crystalline Si substrate, the native oxide layer (~2.5 nm thick), the QL barrier layer (~4.2 nm thick) and the top Cu film, was clearly observed. Although the layered structure of the QL barrier was indistinct, because of the ultra-small thickness of each layer (~1 nm), an alternate bright-and-dark contrast (bright: nitride, containing a large number of light N atoms; dark: heavy metal atoms) could still be identified, revealing the four layers. In the magnified image that is inset in Fig. 1, the as-deposited QL barrier is seen to have an amorphous structure without an ordered lattice; no intermetallic compound or crystalline phase was observed in the amorphous QL barrier, indicating a random solid solution of all incorporated metallic elements and N atoms. Although the metallic elements had different crystal structures and lattice constants, listed in Table 2, they formed a simple solid solution, rather than many separated phases, because of the thermodynamic stability that is provided by the high mixing entropy of the multi-component system [17,18]. Additionally, the severe lattice distortions that are caused by the differences in

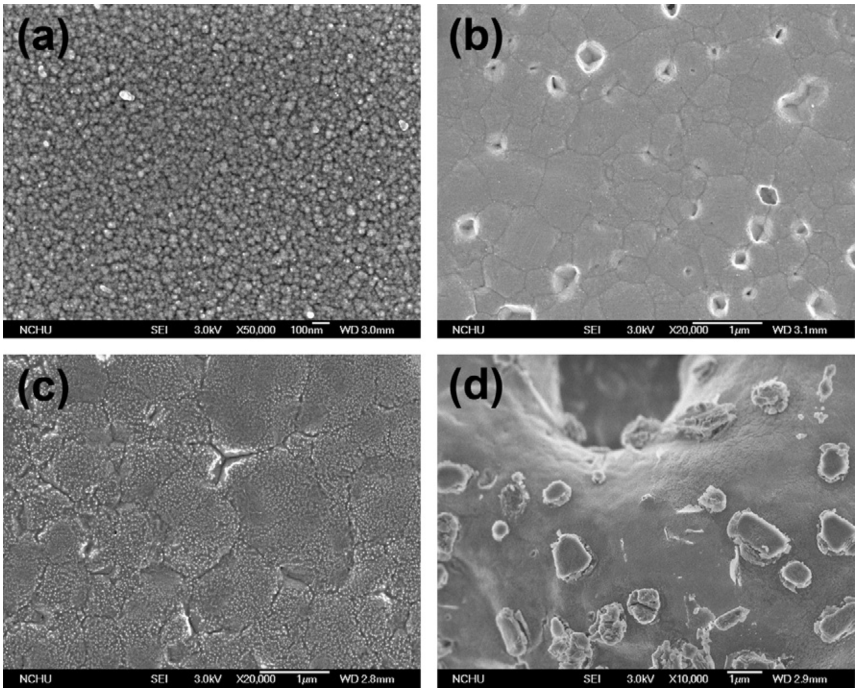

Fig. 2. SEM surface morphologies of (a) as-deposited and (b) 700, (c) 800, and (d) 900 °C annealed Si/QL/Cu film stacks.

Table 1
Chemical compositions of as-deposited (AlCrRuTaTiZr)$N_{0.5}$ senary nitride and AlCrRuTaTiZr senary alloy films, as determined by EPMA.

Element	Al	Cr	Ru	Ta	Ti	Zr	N
Content (at.%)[a] in AlCrRuTaTiZr	10.3	18.8	19.5	17.6	14.9	15.1	–
Content (at.%)[a] in (AlCrRuTaTiZr)$N_{0.5}$	8.8	11.0	11.5	9.5	11.4	10.4	33.2

[a] O contents < 4 at.%.

Table 2
Crystal structures and lattice constants of individual metallic elements in AlCrRuTaTiZr senary alloy and individual nitrides in (AlCrRuTaTiZr)$N_{0.5}$ senary nitride.

Element in AlCrRuTaTiZr	Al	Cr	Ru	Ta	Ti	Zr
Crystal structure[a]	fcc	bcc	hcp	bcc	hcp	hcp
Lattice constant (Å)	4.05	2.89	a: 2.71, c: 4.28	3.30	a: 2.95, c: 4.69	a: 3.23, c: 5.15

Nitride in (AlCrRuTaTiZr)$N_{0.5}$	AlN	CrN	RuN	TaN	TiN	ZrN
Crystal structure[a]	fcc	fcc	fcc	fcc	fcc	fcc
Lattice constant (Å)	4.32	4.14	4.32	4.34	4.24	4.58

[a] fcc: face-centered cubic; bcc: body-centered cubic; hcp: hexagonal close-packed.

the atomic sizes of the incorporated elements, particularly Ru with an extra-large size of 3.56 Å, suppress crystallization during deposition of the film and so cause the formation of the amorphous solid-solution structure.

Fig. 2(a)–(d) shows the SEM surface morphologies of the as-deposited Si/QL/Cu film stack and those annealed at 700–900 °C, respectively. Grain growth of the top Cu films from about 30 nm to 0.5 and 1 μm occurred during annealing at 700 and 800 °C, respectively, associated with the formation of a dense and hexagonal granular structure as well as the elimination of most grain boundaries and possibly other defects. Agglomeration of the Cu films also occurred at high temperatures owing to grain growth and surface tension, and a few small holes were formed at tri-grain junctions because of agglomeration and probably the stresses that were caused by the mismatch between thermal expansion coefficients [21]. Slight oxidation of the Cu film also occurred at 800 °C, forming many small dots on the surface. However, no crystalline phase or faceted compounds formed following annealing at 800 °C, suggesting that the ultrathin QL barrier with a thickness of only 4 nm had a high endurance temperature. At an extremely high temperature of 900 °C, film agglomeration became much more severe, and many faceted compound phases formed, appearing on the roughened film surface, as shown in Fig. 2(d); these were very probably Cu_3Si compounds.

Fig. 3 presents the XRD patterns of as-deposited and thermally annealed Si/QL/Cu film stacks, which confirmed the conclusions drawn from the above SEM observations. In the diffraction pattern of the as-deposited film stack, three main but broad peaks at 43.3°, 50.4° and 74.1°, corresponding to the (1 1 1), (2 0 0) and (2 2 0) lattice planes, respectively, of face-centered cubic Cu, revealed the low crystallinity and small grain sizes of the as-deposited Cu film. Following annealing at 700 or 800 °C, similar but sharpened peaks with increased intensities and smaller full widths at half maxima appeared, consistent with the observations of the grain growth of the Cu films. No other crystalline compound phase was formed in the annealed samples, suggesting the high resistance of the ultrathin QL barrier to the interdiffusion of Cu and Si. Only at 900 °C, the formation of Cu_3Si compound phase with two clear diffraction peaks at 44.7° and 45.3° indicated the interdiffusion through the barrier at extremely high temperature and the failure of the QL barrier, as observed in the SEM image in Fig. 2(d).

Fig. 4 plots the change in the measured sheet resistance of Si/QL/Cu film stacks after annealing at high temperatures. Clearly, the sheet resistance of the film stack fell from 0.37 to around 0.05 Ω/□ after annealing at 700 and 800 °C because of the apparent grain growth of the Cu films and the elimination of most grain boundaries and defects. Annealing at 900 °C caused the sheet resistance to jump to 267 Ω/□, simply because of agglomeration of the Cu film, the interdiffusion of Cu and Si and the formation of many Cu_3Si compounds, owing to the failure of the QL

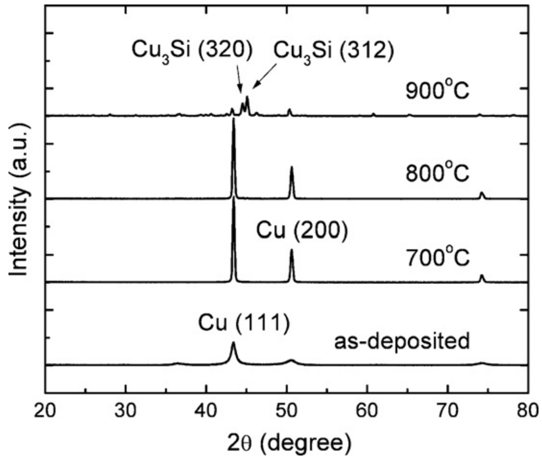

Fig. 3. XRD patterns of as-deposited and 700, 800, and 900 °C annealed Si/QL/Cu film stacks.

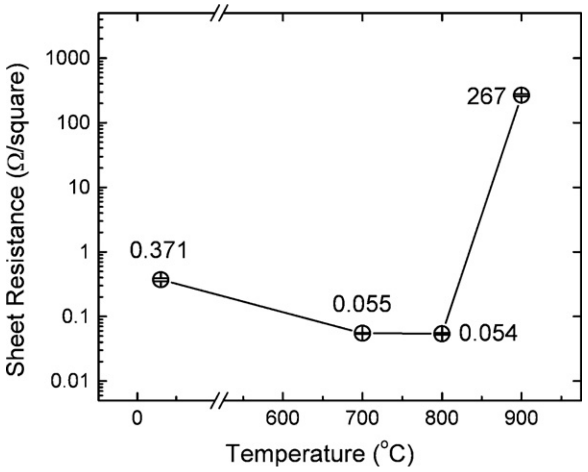

Fig. 4. Sheet resistance of as-deposited and 700, 800, and 900 °C annealed Si/QL/Cu film stacks.

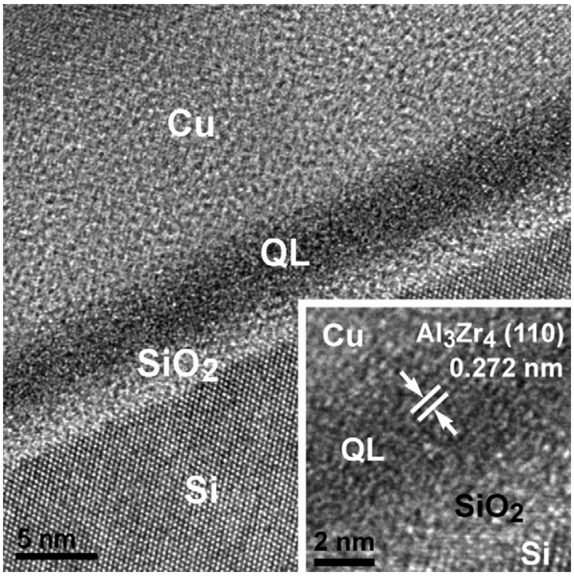

Fig. 5. HRTEM image of 800 °C-annealed Si/QL/Cu film stack (insert: magnified image around QL barrier).

barrier. These findings were consistent with the SEM and XRD analyses.

Fig. 5 presents the HRTEM image of the Si/QL/Cu film stack that was annealed at 800 °C. As in the as-deposited stack in Fig. 1, the stacked structure that had been annealed at high temperature still exhibited the single-crystalline Si substrate, the native oxide, the QL barrier and the top Cu film, and had clear interfaces. Neither Cu silicide nor any other compound was formed in the Si substrate, and neither the QL barrier nor the native oxide was damaged, suggesting the apparently effective retardation of diffusion of Cu atoms by the QL barrier. Only the alloying (mixing) of the nitride and the metallic layers was expected to yield an unclear layered structure of the QL barrier, with the loss of the original alternate bright-and-dark contrast. Fortunately, the QL barrier retained an amorphous structure after annealing, revealing the high thermal stability of the present developed barrier material. The amorphous matrix contained only a few nanocrystallites with unclear ordered lattices, as seen in the inset magnified image; the interplanar spacing of 0.27 nm corresponded to an Al_3Zr_4 (1 1 0) lattice and revealed the possibility of crystallization of the amorphous structure into intermetallic compounds, because the QL barrier comprised both AlCrRuTaTiZr alloy and $(AlCrRuTaTiZr)N_{0.5}$ unsaturated nitride.

The above analyses indicate that the multi-component and multilayer structure with a thickness of only 4 nm thick effectively inhibits the interdiffusion of Cu and Si during thermal annealing at 800 °C, and can be utilized as a robust barrier layer in Cu interconnects of the sub-32 nm manufacturing generation. Although the temperatures in the backend processes or operations of integrated circuits never exceed 400 or 200 °C, respectively, however, it is understood that from the aspect of reliability a higher endurance temperature in a conventional thermal annealing test simply indicates a longer lifetime in a low-temperature environment. To date, no other comparable barrier material with the ultra-small thickness (4 nm) and with a high soaking temperature (800 °C) and a long soaking duration (30 min) has been reported. The following important factors related to the superior performance of the present QL barrier are suggested:

(1) Thermodynamic: the high mixing entropy of a multi-component system results in the formation of a high thermally stable simple solid solution with a random amorphous structure which has relatively few viable diffusion paths.
(2) Structural: the high packing factor that is attributed to the addition of differently sized atoms reduces free volume and the molar volume of vacancies for Cu atoms to diffuse.
(3) Kinetic: the severe lattice distortions that are caused by the incorporation of multi-principal elements of various atomic sizes increase the activation energy of crystallization and diffusion and reduce the diffusion coefficients of Cu atoms.
(4) Geometrical: the interface lattice mismatch in the multilayered structure increases the probability of lateral diffusion along those interfaces and increases diffusion distance.

4. Conclusions

In this study, a quaternary-layered structure of alternate $(AlCrRuTaTiZr)N_{0.5}$ senary nitride and AlCrRuTaTiZr senary alloy with a thickness of only 4 nm was developed as a robust diffusion barrier for advanced Cu interconnects. Experimental results indicate that the quaternary-layered barrier effectively retarded the interdiffusion of Cu and Si during annealing at a high temperature of 800 °C, without the formation of any Cu silicides. This finding suggests the high endurance temperature and potential of the presented barrier material for practical use in Cu interconnects of the sub-32 nm manufacturing generation. Important factors include a simple amorphous solid-solution structure, attributed to multi-component addition, a low free volume and severe lattice distortions that are caused by the differently sized atoms, and elongated diffusion paths through the multilayer structure.

Acknowledgements

The authors gratefully acknowledge financial support for this research by the National Science Council, Taiwan, under grant no. NSC-100-2628-E-005-006-MY3, and by the Ministry of Education, Taiwan, under the ATU plan.

References

[1] J.D. McBrayer, R.M. Swanson, T.W. Sigmon, J. Electrochem. Soc. 133 (1986) 1242–1246.
[2] C.A. Chang, J. Appl. Phys. 67 (1990) 566–569.
[3] A.E. Kaloyeros, E. Eisenbraun, Annu. Rev. Mater. Sci. 30 (2000) 363–385.
[4] T. Kouno, H. Niwa, M. Yamada, J. Electrochem. Soc. 145 (1998) 2164–2167.
[5] M.H. Tsai, S.C. Sun, C.E. Tsai, S.H. Chuang, H.T. Chiu, J. Appl. Phys. 79 (1996) 6032–6938.
[6] Y. Liu, S. Song, D. Mao, H. Ling, M. Li, Microelectron. Eng. 75 (2004) 309–312.
[7] S.H. Kwon, O.K. Kwon, J.S. Min, S.W. Kang, J. Electrochem. Soc. 153 (2006) G578–G581.
[8] S. Rawal, D.P. Norton, H. Ajmera, T.J. Anderson, L. McElwee-White, Appl. Phys. Lett. 90 (2007) 051913.
[9] C.W. Chen, J.S. Chen, J.S. Jeng, J. Electrochem. Soc. 155 (2008) H438–H442.
[10] P. Majumder, C. Takoudis, Nanotechnology 19 (2008) 205202.
[11] L.C. Leu, D.P. Norton, L. McElwee-White, T.J. Anderson, Appl. Phys. Lett. 92 (2008) 111917.
[12] X.P. Qu, J.J. Tan, M. Zhou, T. Chen, Q. Xie, G.P. Ru, B.Z. Li, Appl. Phys. Lett. 88 (2006) 151912.
[13] Q. Xie, Y.L. Jiang, J. Musschoot, D. Deduytsche, C. Detavernier, R.L. Van Meirhaeghe, S. Van Den Berghe, G.P. Ru, B.Z. Li, X.P. Qu, Thin Solid Films 517 (2009) 4689–4693.
[14] S.H. Kim, H.T. Kim, S.S. Yim, D.J. Lee, K.S. Kim, H.M. Kim, K.B. Kim, H. Sohn, J. Electrochem. Soc. 157 (2008) 589–594.
[15] J. Koike, M. Wada, Appl. Phys. Lett. 87 (2005) 041911.
[16] A.M. Caro, S. Armini, O. Richard, G. Maes, G. Borghs, C.M. Whelan, Y. Travaly, Adv. Funct. Mater. 20 (2010) 1125–1131.
[17] J.W. Yeh, S.K. Chen, S.J. Lin, J.Y. Gan, T.S. Chin, T.T. Shun, C.H. Tsau, S.Y. Chang, Adv. Eng. Mater. 6 (2004) 299–303.
[18] J.W. Yeh, S.K. Chen, J.Y. Gan, S.J. Lin, T.S. Chin, T.T. Shun, C.H. Tsau, S.Y. Chang, Metall. Mater. Trans. A 35 (2004) 2533–2536.
[19] J.W. Yeh, S.Y. Chang, Y.D. Hong, S.K. Chen, S.J. Lin, Mater. Chem. Phys. 103 (2007) 41–46.
[20] S.Y. Chang, M.K. Chen, D.S. Chen, J. Electrochem. Soc. 156 (2009) G37–G42.
[21] S.Y. Chang, D.S. Chen, Appl. Phys. Lett. 94 (2009) 231909.
[22] S.Y. Chang, D.S. Chen, J. Electrochem. Soc. 157 (2010) G154–G159.